PAPER • OPEN ACCESS

Human-caused ocean warming has intensified recent hurricanes

View the article online for updates and enhancements.

ENVIRONMENTAL RESEARCH
CLIMATE

PAPER

Human-caused ocean warming has intensified recent hurricanes

Daniel M Gilford[*] , Joseph Giguere and Andrew J Pershing

Climate Central, Inc., Princeton, NJ, United States of America
[*] Author to whom any correspondence should be addressed.

E-mail: dgilford@climatecentral.org

Abstract

Understanding how rising global air and sea surface temperatures (SSTs) influence tropical cyclone intensities is crucial for assessing current and future storm risks. Using observations, climate models, and potential intensity theory, this study introduces a novel rapid attribution framework that quantifies the impact of historically-warming North Atlantic SSTs on observed hurricane maximum wind speeds. The attribution framework employs a storyline attribution approach exploring a comprehensive set of counterfactuals scenarios—estimates characterizing historical SST shifts due to human-caused climate change—and considering atmospheric variability. These counterfactual scenarios affect the quantification and significance of attributable changes in hurricane potential and observed actual intensities since pre-industrial. A summary of attributable influences on hurricanes during five recent North Atlantic hurricane seasons (2019–2023) and a case study of Hurricane Ian (2022) reveal that human-driven SST shifts have already driven robust changes in 84% of recent observed hurricane intensities. Hurricanes during the 2019–2023 seasons were 8.3 m s^{-1} faster, on average, than they would have been in a world without climate change. The attribution framework's design and application, highlight the potential for this framework to support climate communication.

1. Introduction

Rising global mean air temperatures and sea surface temperatures (SSTs) are expected to influence tropical cyclone activity throughout the 21st century (Sobel *et al* 2016, Collins *et al* 2019). Hurricane intensity changes, in particular, are important to understand and elucidate because they are a key driver of storm risks and damages in the United States (e.g. Schmidt *et al* 2009, Nordhaus 2010, Emanuel 2011). In this study we present a novel rapid attribution framework that quantifies how historical increases in North Atlantic SSTs drive attributable changes in observed hurricane intensities.

Theory and numerical modeling indicate human-caused climate change should strengthen hurricane intensities on average (Emanuel 2005, Schiermeier 2008, Sobel *et al* 2016, Murakami *et al* 2020). Wehner and Kossin (2024) showed that anthropogenic global warming has already increased the likelihoods of extremely intense (>86 m s^{-1}) tropical cyclone potential intensities (PI; i.e. the theoretical maximum intensity of a storm given its environment). Higher PI values mean the theoretical maximum speed limits over the Atlantic have increased, permitting individual storms to reach higher wind speeds in today's warmer climate. Observational evidence corroborates this theory: the frequency of major hurricanes (category 3+) has increased since 1979 (Elsner *et al* 2008, Holland and Bruyère 2014, Kossin *et al* 2020). But when a real-world storm develops and threatens a coastline, to what extent is its maximum wind speed attributable to human influences?

Connecting these dots is critical for climate communication. Hurricanes—especially landfalling hurricanes with high intensities—can act as 'focusing events' that draw public attention (Birkland 1998, Arnold *et al* 2021, Silver and Jackson 2023). Increased attention during and in wake of storms creates opportunities for public and private discourse around climate and disaster preparedness (Cody *et al* 2017,

Wong-Parodi and Garfin 2022). Climate change attribution plays an important role in these discussions. Social studies have shown that personal experiences with extreme weather and attribution messaging both have strong potential to influence public perceptions of climate risk and decision-making (Ogunbode *et al* 2019, Boudet *et al* 2020, Osaka and Bellamy 2020, Ettinger *et al* 2021, McClure *et al* 2022, Thomas-Walters *et al* 2024, Zanocco *et al* 2024). Presenting scientifically-sound estimates, and carefully, deliberately conveying methodologies can be effective for attribution-driven climate communication (Osaka and Bellamy 2020, Ettinger *et al* 2021, van Oldenborgh *et al* 2021, Thomas-Walters *et al* 2024).

Rapid attribution systems designed and used to produce these estimates can also help the research community identify which events/conditions are unusual and warrant closer study (Swain *et al* 2020, Gilford *et al* 2022). Today, timely attribution studies of extreme temperatures and other weather events are routinely performed with peer-reviewed methods and delivered by World Weather Attribution (e.g. Philip *et al* 2020), Climate Central (Gilford *et al* 2022), and others. But key for such messaging is a pre-existing attribution system that can rapidly and reliably estimate climate's influence on particular events.

While formal extreme event attribution science has become mature in recent decades (e.g. National Academies of Sciences 2016, Philip *et al* 2020), hurricane attribution science is still relatively nascent and challenging (Seneviratne *et al* 2021). There is strong evidence from hurricane modeling and 'storyline' attribution (see below) that rainfall intensity and accumulation have already increased by ~10% or more for many individual storms (Van Oldenborgh *et al* 2017, Trenberth *et al* 2018, Wang *et al* 2018, Reed *et al* 2021, Reed and Wehner 2023). Attributable damages from hurricanes have also been explored (Strauss *et al* 2021, Wehner and Reed 2022). Meanwhile, high-resolution model simulations project that future storm intensities should increase with ongoing global warming, but suggest anthropogenic influences on recent storms are not yet strong enough to be significant (Lackmann 2015, Patricola and Wehner 2018, Wehner *et al* 2019). In contrast, Pfleiderer *et al* (2022) used a statistical emulator to show that human influences recently elevated Atlantic SSTs, making the 2020 hurricane season anomalously active, despite offsets from interannual variability in atmospheric circulation. They found that 'SSTs over the MDR [main development region] contain relevant information' for estimating attributable hurricane activity in the North Atlantic.

Thus to calculate the influence of human-caused climate change on hurricane intensities, one must first assess how climate change has influenced SSTs. Specifically, it is critical to obtain or determine a 'counterfactual' estimate of what SSTs might be in our modern world without anthropogenic emissions—an approach commonly used in climate attribution science. In this study we use results from a recent comprehensive study of historically attributable ocean temperatures (Giguere *et al* 2024) to derive a counterfactual scenario of what North Atlantic SSTs would be in the absence of human-caused global warming. We also consider a suite of additional counterfactual scenarios, with a range of physical and statistical assumptions to evaluate attribution uncertainties.

Potential intensity theory (e.g. Emanuel 1987, Bister and Emanuel 1998) makes the connection between SSTs and intensities explicit by assuming tropical cyclones operate like heat engines, tying a storm's potential maximum to the storm's efficiency and fuel availability (i.e. from ocean heat). Changes in the distribution of actual storm lifetime maximum intensities have a strong empirical relationship with changes in potential intensity (e.g. Emanuel 2000, Sobel *et al* 2016, Gilford *et al* 2019, Sparks and Toumi 2024, Wehner and Kossin 2024). We leverage this statistical relationship to estimate how a storm's observed actual intensity (AI) might respond to PI changes that are, in turn, driven by attributable changes in ocean temperatures.

In this study we develop an attribution framework to assess how SSTs made warmer by climate change are influencing observed hurricane intensities. The framework is designed to underpin a rapid attribution system for deployment shortly after a hurricane event, with results communicated through trusted messengers to the public. In section 2 we describe the approach, data, models, and theory of the attribution framework. Section 3 shows attribution estimates for SSTs, potential intensity, and AI. Included are two real-world applications of the framework: estimates of SST-driven attributable intensities over the last five North Atlantic hurricane seasons (2019–2023) and a case study of Hurricane Ian (2022). Study implications and limitations are discussed in the context of our existing scientific understanding in section 4. Finally, we summarize our key findings in section 5.

2. Data & methods

2.1. Attribution framework overview

Here we briefly describe the assumptions and scope of the attribution framework. It is designed to rapidly estimate modern attributable changes in hurricane intensities contributed by human-driven SST changes (figure 1). Sections that follow detail the data and methodologies of each framework component.

We focus our study on the North Atlantic basin (9° N–60° N, 100–20° W). All climatologies and anomalies are calculated relative to the 1991–2020 period. Study quantities are computed over a range time
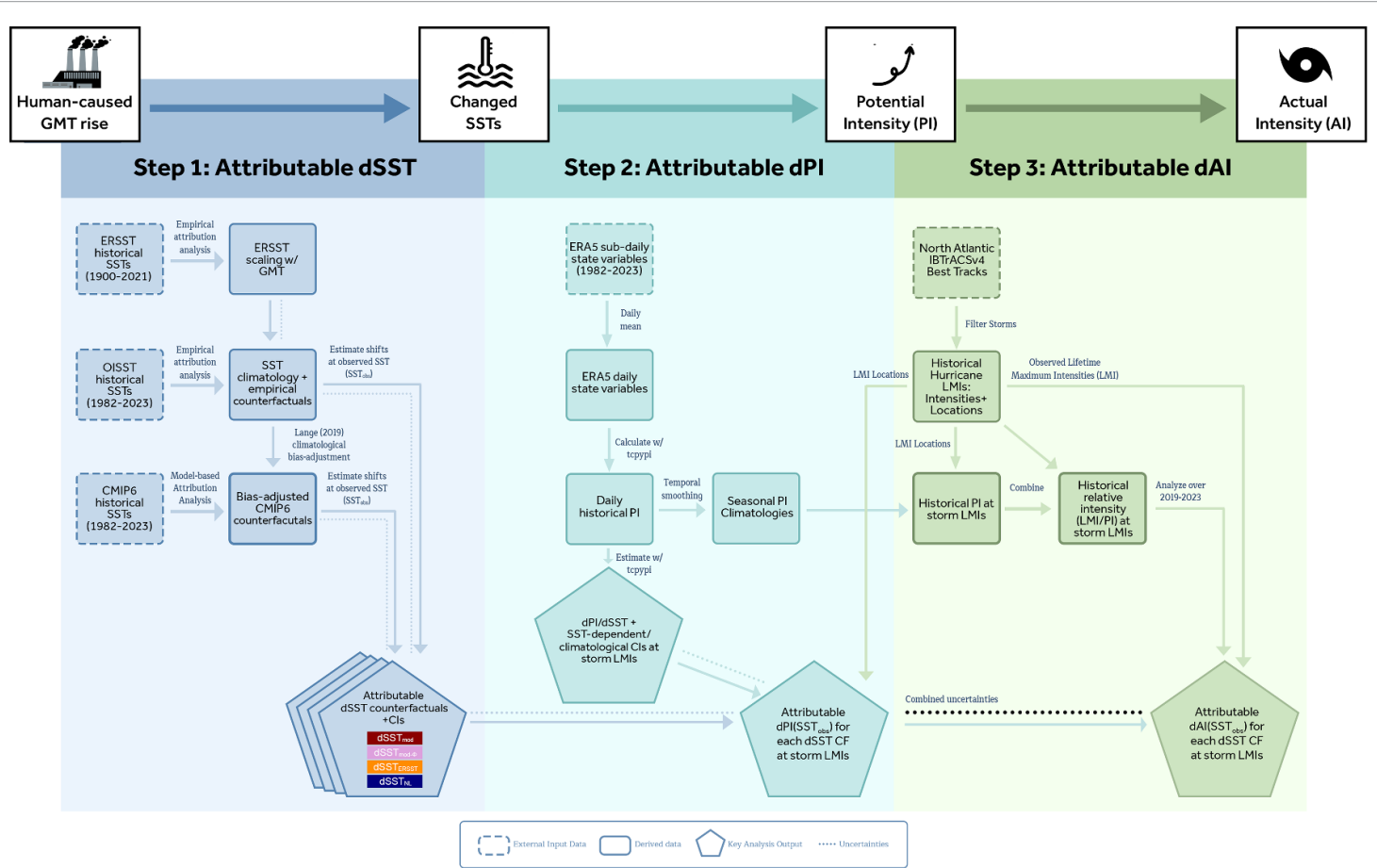
Figure 1. Components, methodology, and flow of the SST-driven tropical cyclone intensity attribution framework. CI = confidence interval; CF = counterfactual.

Table 1. Study counterfactual scenarios of attributable changes in North Atlantic basin SSTs.

Symbol	Name	Counterfactual Description	Color
$dSST_{mod}$	Modern	Shifts from [G24, GMT] regression (1982–2021)	Dark Red
$dSST_{mod\text{-}\phi}$	Modern zonal-mean	Zonal-mean shifts from [G24, GMT] regression (1982–2021)	Purple
$dSST_{ERSST}$	ERSST	Shifts from [ERSST, GMT] regression (1900–2021)	Orange
$dSST_{NL}$	Nonlocally- damped modern	$dSST_{mod}$ minus fractional nonlocal tropical influences (after Swanson 2008)	Navy Blue

periods created by subdividing each year into 31-day bi-monthly periods (labeled t_{bm}) of ± 15 days centered on the 1st and 15th of each month (i.e. 12 periods between 1 June–15 November). These approximately month-long periods are consistent with analyses of previous studies linking observed intensities to PI (Emanuel 2000, Wing *et al* 2015, Gilford *et al* 2019, Sparks and Toumi 2024). In particular, mean analyses over t_{bm} filters out high-frequency atmospheric noise, as well as storm influences on their own environments, yielding more representative estimates of the SSTs and PI each storm experiences. Meanwhile, the range of PI sensitivities across t_{bm} provides a basis for estimating what uncertainties variable environmental conditions might contribute to attribution (see section 2.3).

Climate attribution compares an event in a current human-influenced climate with a simulated outcome in an alternative climate—a counterfactual—without anthropogenic forcing. In this study we use 'counterfactual scenario' to refer to different constructed representations of these simulated outcomes. We adopt a storyline attribution approach (Shepherd 2016, Lloyd and Oreskes 2018, Shepherd *et al* 2018), considering multiple counterfactual scenarios to estimate the attributable shifts[1] in SST (dSST, °C) across the North Atlantic since pre-industrial. Counterfactual scenario dSSTs are derived from the methods and results of Giguere *et al* (2024) by computing the temperature change between counterfactual and observed modern distributions with SSTs that are representative of the seasonal and location-specific conditions at each storm's lifetime maximum intensity (section 2.2).

Attributable SST changes are used to determine the associated attributable changes in hurricane potential intensity (e.g. Emanuel 1986). We characterize and exploit strong linear relationships between SSTs and PI changes to calculate PI shifts attributable to the set of counterfactual scenario SST shifts (dPI, in m s^{-1}). Relying on the historically robust statistical relationship between observed AI and PI (Emanuel 2000, Gilford *et al* 2019, Sparks and Toumi 2024), we use the SST-driven attributable dPI to estimate historically attributable AI shifts (dAI, in m s^{-1}). Attributable PI and AI changes are estimated at the time, location, and wind speed of a storm's lifetime maximum intensity (as defined in section 2.4.1).

We present intensity attribution estimates for Atlantic hurricanes over 2019–2023 to demonstrate the attribution system's design, development, and implementation with real storms.

2.2. SST attribution

Our data and models are based in part on the published analyses of Giguere *et al* (2024, hereafter G24, their figure 1) which adapts established attribution protocols and techniques (Philip *et al* 2020, Gilford *et al* 2022). We combine statistics, simulated SSTs from the Coupled Model Intercomparison Project Phase 6 (CMIP6; Eyring *et al* 2016), and observations from the Optimum Interpolation SST version 2 (OISST; Reynolds *et al* 2002) into a multi-method approach to attribute historical SST changes to human-caused climate change.

For each observed SST (SST_{obs}) in the record, we find its associated quantile in the observed distribution, and then resample that quantile on the counterfactual distribution to compute a counterfactual SST. We then compute dSSTs, defining them as the difference between SST_{obs} and the counterfactual SST at the location and during the time period (t_{bm}) of each storm's analyzed lifetime maximum intensity (section 2.4.1). This follows a storyline approach for attribution (e.g. Shepherd *et al* 2018) by focusing on the magnitude of dSSTs across each counterfactual scenario, rather than on the changes in likelihood associated with SST_{obs} across scenarios. This framing allows us to calculate and assess the attributable dPI and dAI responses for each scenario and their uncertainties individually, disambiguating how each representation of attributable SSTs might have effectively influenced historical hurricane intensities (sections 2.3 and 2.4).

We develop and apply four different SST counterfactual scenarios to estimate and bound their historical contributions to attributable changes in contemporary Atlantic hurricane intensities (table 1). Each scenario characterizes how storm environments have changed historically; they span a range of assumptions about

---

[1] These attributable 'shifts' in the attributed variable's native unit are often technically referred to as attributable 'intensities' in climate attribution literature. We use 'shifts' throughout to avoid confusion with our subject, hurricane intensities.

how and to what extent human-caused SST warming has historically influenced AI. The scenarios are Modern, Zonal-mean Modern, ERSST, and Nonlocally-damped Modern; each is described below.

Modern ($dSST_{mod}$): This is the baseline scenario directly implementing G24's OISST approach. Empirical- and model-derived attributable dSSTs are averaged together to produce a set of best estimate counterfactual shifts over the North Atlantic basin. The empirical observation-based approach analyzes the linear relationships between the 3-year running average of global mean temperature (GMT) and local observed temperatures from OISST to produce empirical modern and counterfactual distributions.

Observation-based SST distributions are constructed by first regressing the local timeseries of median or quantile SSTs (over each t_{bm}) against GMT over 1982–2023. These distributions are then shifted using their linear relationships and the observed attributable GMT change since pre-industrial ($+1.2\,^{\circ}$C as of 2021, Eyring *et al* 2021), either uniformly across the distribution (i.e. 'median method' in Gilford *et al* 2022) or quantile-by-quantile to allow for historical variance changes ('quantile method'). Counterfactual distributions resulting from the median and quantile methods are equally weighted and resampled to produce a single observation-based dSST value for each observed SST_{obs} in the OISST dataset. Observation-based dSST uncertainties are estimated with the 95% confidence interval given by the standard error from the GMT and median SST timeseries regression.
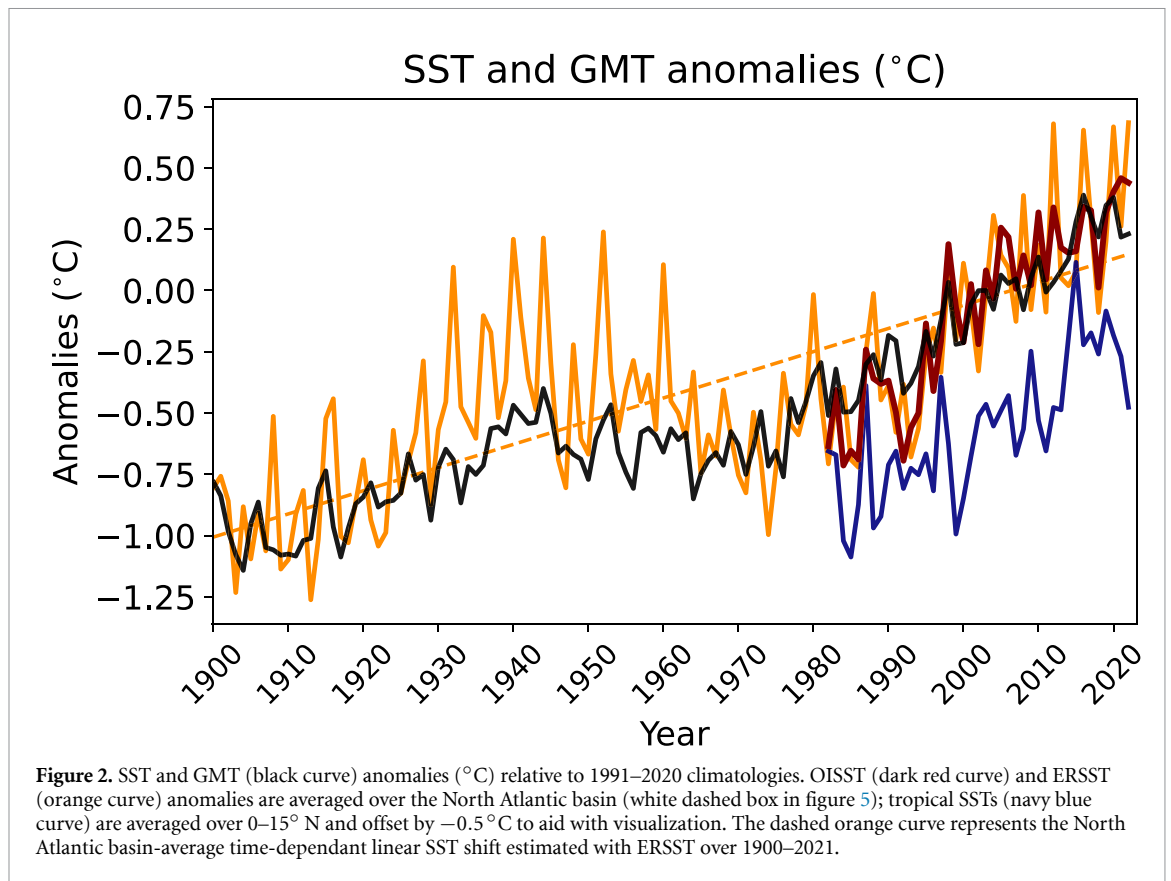
Modeled SST distributions are produced from 13 CMIP6 pairs of historical+forced and pre-industrial control simulations over 1900–2050 (supporting table S1). Model SSTs are bias-adjusted against the OISST climatology over 1991–2020 following Lange (2019) and regridded to a common $1.5^{\circ} \times 1.5^{\circ}$ grid (Zhuang *et al* 2023, following G24). Each model's counterfactual distribution is taken from its pre-industrial control simulation, while simulated modern distributions are estimated from the 31-year period centered on the year each model crossed $+1.2\,^{\circ}$C GMT (relative to control). The 13 model-pair attributable shift estimates are averaged to produce a single model-based dSST value for each observed SST_{obs}. Model-based dSST uncertainties are estimated with the 95% confidence interval of the inter-model spread.

Finally, the observation- and model-based dSSTs are averaged together to produce a synthesized set of 'Modern' scenario of SST counterfactual shifts ($dSST_{mod}$) for each t_{bm} and location in the North Atlantic basin. dSST uncertainties from models and observations are added together in quadrature, conservatively assuming they are independent.

Zonal-Mean Modern ($dSST_{mod-\phi}$): This scenario considers how hurricanes might respond if the portion of local SSTs attributable to greenhouse gas emissions was zonally-distributed across the globe, smoothing out the influences of regional climate variability. We take the zonal mean across globally-resolved $dSST_{mod}$ at each latitude to find the set of dSSTs for each t_{bm} and location in the North Atlantic basin. Departures from the zonal mean are interpreted as being driven by local forcing factors such as multi-decadal changes in ocean circulation or aerosol forcing and feedbacks (e.g. Knutson *et al* 2019, Rousseau-Rizzi and Emanuel 2021, see section 4).

ERSST ($dSST_{ERSST}$): This scenario uses a longer (1900–2021) but coarser (monthly at $2^{\circ} \times 2^{\circ}$ resolution) SST dataset to estimate the historical SST-GMT relationships; the approach reduces the influence of interannual variability at the expense of resolution. We employ the empirical observation-based median-method to derive attributable shifts from the Extended Reconstructed SST Version 5 (ERSST; Huang *et al* 2015, 2017). While coarser and having higher temporal variance in its early record, ERSST has the advantage of providing SSTs back to 1900 when attributable GMT was $\sim0\,^{\circ}$C (Masson-Delmotte *et al* 2021). Figure 2 shows the best-fit line from a regression between a 3-year running mean of annual GMT and ERSSTs averaged over the North Atlantic main development region (box in figure 4); they share a robust, upward trend. Importantly, this long-term congruence considers changes before the potentially confounding effects of human-emitted aerosols (e.g. Evan *et al* 2009). Our study does not explicitly separate human-emitted aerosols from the covarying human emissions of greenhouse gases (e.g. Knutson *et al* 2019, Trenary *et al* 2019, Rousseau-Rizzi and Emanuel 2021). Note that the SST rebound in the era after the aerosol loading peak (late $\sim$1970s) is not excluded from the Modern scenario definition above. However, the ERSST scenario estimates SST changes associated with anthropogenic emissions over a longer period—long enough to incorporate and bypass the rise and fall of human-emitted aerosol effects on North Atlantic SSTs.

Nonlocally-damped Modern ($dSST_{NL}$): This scenario estimates how nonlocal atmospheric influences might damp the influence of attributable dSSTs on PI. At each t_{bm} and location in the North Atlantic basin we construct and compute a linear adjustment to $dSST_{mod}$ to quantify this effect. Local SST changes are the strongest driver of local PI changes (see sensitivity calculations, section 2.3). But previous studies have shown that when local SSTs increase on long timescales, a nonlocal atmospheric response across the tropics can simultaneously increase upper tropospheric temperatures, affect moisture profiles, and/or affect surface winds, potentially depressing the overall impact of SST changes on local PI (e.g. Shen *et al* 2000, Swanson 2008, Vecchi *et al* 2008, Emanuel *et al* 2013). Rather than modeling these nonlocal effects explicitly by adjusting environmental profiles or PI input parameters—which our univariate attribution approach does

Figure 2. SST and GMT (black curve) anomalies (°C) relative to 1991–2020 climatologies. OISST (dark red curve) and ERSST (orange curve) anomalies are averaged over the North Atlantic basin (white dashed box in figure 5); tropical SSTs (navy blue curve) are averaged over 0–15° N and offset by −0.5 °C to aid with visualization. The dashed orange curve represents the North Atlantic basin-average time-dependant linear SST shift estimated with ERSST over 1900–2021.

not permit—we instead remove an estimated magnitude of the nonlocal influence from the Modern scenario up front (treating the Modern counterfactual as a baseline), before computing attributable intensity changes with the damped SST changes. The resulting $dSST_{NL}$ quantifies a first order estimate of how a nonlocal atmospheric response to climate warming might limit how representative dSSTs affect attributable PI (and hence attribitable AI) results. We apply the simple linear damping methodology of Swanson ([2008](#)), their equation (2):

$$dSST_{NL} = dSST_{mod} - \alpha * dSST_{tropics} \tag{1}$$

where we calculate the coefficient for the tropical mean contribution, $\alpha = 0.46$, by maximizing a correlation between the traditional main development region PI and SST anomalies over 1980–2023; we find very similar results despite differences in data sources, PI calculations, and the time range of our data being updated through present (supporting figure S1). $dSST_{tropics}$ is given by the average of $dSST_{mod}$ over 0–15° N; over 2019–2023, $dSST_{tropics} = 0.99\,°C$, so that $dSST_{NL}$ is on average $\sim 0.46\,°C$ less than $dSST_{mod}$ (cf figure [3](#)). Note that other tropical bands were considered (0–20° N, 0–25° N, 20° S–20° N) to account for tropical expansion, but yielded lower correlations. While we have grounded this study's analysis in the simple linear expression of equation ([1](#)), more complicated depictions of nonlocal damping could be considered in the future to yield a broader plausible range for this counterfactual.

2.3. Potential intensity attribution

2.3.1. Historical potential intensity analysis

Historical daily potential intensities (e.g. Emanuel [1986](#), Bister and Emanuel [1998](#), [2002](#)) are computed with the 'tcpypi' algorithm (Gilford [2020](#), Gilford [2021](#)). The algorithm calculates PI (in m s^{-1}) using environmental state variables as inputs: SST, mean sea level pressure, and atmospheric profiles of temperature and water vapor; algorithm parameter values are left at the tcpypi defaults. Historical 6-hourly state variables (SST; p_{msl}; $T(p)$ and $q(p)$ on 28 pressure levels over 1000–70 hPA) are drawn from the fifth generation ECMWF atmospheric reanalysis (ERA5) downloaded from An Analysis-Ready Cloud-Optimized Reanalysis Dataset (Carver and Merose [2023](#)) (ARCO-ERA5, *accessed 1 April 2024*) and averaged to daily timesteps over 1982–2023 at 0.25° × 0.25° resolution, and then are grouped by each t_{bm} for sensitivity and attribution analyses. Climatological (1991–2020) SSTs, and algorithm output PI, outflow temperatures, and

outflow levels analyzed at each t_{bm} are consistent with published TC PI climatologies (supporting figure S3, Gilford *et al* 2017).

2.3.2. Estimating dPI

We determine PI sensitivities to local attributable SST changes with an empirical approach. At each location and t_{bm}, the distribution of SST-driven PI changes (dPI) is approximated with the linear model:

$$\text{dPI} = \frac{\text{dPI}}{\text{dSST}} * \text{dSST} \tag{2}$$

where dSST are the counterfactual shifts in °C and their uncertainties (section 2.2; table 1) and $\frac{\text{dPI}}{\text{dSST}} \sim f(\tilde{\mu}, \sigma_{\text{lower}}, \sigma_{\text{upper}})$ is the distribution of PI linear sensitivities (with median, $\tilde{\mu}$, and [lower; upper] bounded confidence intervals [$\sigma_{\text{lower}}; \sigma_{\text{upper}}$]) to changes in SSTs. Sensitivity distributions are compiled by fitting the model's slope to outputs from empirical simulations: at each storm's lifetime maximum intensity location and for each day over the storm's climatological t_{bm} periods (1991–2020, state variables from 930 total daily environments per bi-monthly period), we recompute potential intensities after adding progressive 0.25 °C steps to the observed SST, with steps ranging over $-1.25\,°\text{C} \rightarrow +1.25\,°\text{C}$ (~maximum median dSST across counterfactual scenarios). During each daily sensitivity computation the other environmental conditions (T and q profiles, p_{msl}) remain fixed at their daily values.

2.4. AI attribution

2.4.1. Hurricane track data & lifetime maximum intensity

We illustrate the attribution framework by applying it to historical tropical cyclones at their lifetime maximum intensities, over the five year period 2019–2023. Observed tropical cyclone best track data are drawn from the International Best Track Archive for Climate Stewardship version (IBTrACS; Knapp *et al* 2010, 2018); best tracks provide the 6-hourly mean positions (longitude, latitude) and maximum sustained wind speeds for each storm in the North Atlantic basin over 2019–2023.

Following the approach described by Gilford *et al* (2019, their section 2b) observed storms are filtered for eligibility. We seek to apply potential intensity theory at the time and location of an analysis-appropriate wind speed maximum along each storm's track (see Emanuel 2000).

We first consider all storms that attained at least hurricane wind speeds ($>32\,\text{m s}^{-1}$) at some (6-hourly) point along their track within the bounds of the North Atlantic basin. We define each storm's 'analysis lifetime maximum intensity' (hereafter just LMI)—indexing each storm's time, position, and AI—as the first 6-hourly step when the storm attains its lifetime maximum. If this step's storm position is over land but the previous 6-hourly step is over ocean, we instead take that previous step's time, position, and intensity as the storm's LMI. Storms with a lifetime maximum over land for $>6\,\text{h}$ are considered ineligible for PI theory application, and are removed from the dataset. Likewise, we remove storms which had their lifetime maximum intensity abruptly limited by coincidental passage over cold ocean temperatures. After filtering and identifying storm LMIs, 38 total storms remain for attribution analysis over the 2019–2023 North Atlantic hurricane seasons.

2.4.2. Relative intensity & estimating attributable AI

We use attributable potential intensity changes to estimate AI changes through their established along-track statistical relationship. The relative intensity of a hurricane at its LMI, $\nu = \frac{\text{AI}}{\text{PI}}$, describes the fractional portion of PI that a storm achieves during its lifetime (e.g. Emanuel 2000). The historical distribution of relative intensity is uniform; this a robust feature across the literature, indicating that the probability of a storm achieving any intensity is equally distributed between a lower bound of marginal hurricane wind speeds (~$33\,\text{m s}^{-1}$) and an upper bound given by its local PI (Emanuel 2000, Zeng *et al* 2007, Swanson 2008, Sobel *et al* 2016, Gilford *et al* 2019, Sparks and Toumi 2024). The key property of this distribution for our purposes is that, if this relationship holds under climate change, then any permanent shift in the distribution of along-track PI will be accompanied by a similiar shift in AI (e.g. Sobel *et al* 2016, their supplementary materials). In this study we assume the relationship has held (i.e. ν has remained fixed) over the period of anthropogenic forcing, so that when modern observed storms occur they follow the climatological ν distribution, and,

$$\nu_{\text{mod}} = \nu_{cf} \rightarrow \frac{\text{AI}_{\text{mod}}}{\text{PI}_{\text{mod}}} = \frac{\text{AI}_{cf}}{\text{PI}_{cf}} \tag{3}$$

for any given storm along its track. Recognizing $\text{dPI} \equiv \text{PI}_{\text{mod}} - \text{PI}_{cf}$ and $\text{dAI} \equiv \text{AI}_{\text{mod}} - \text{AI}_{cf}$, we solve for the counterfactual AI and the accompanying attributable change in AI in terms of modern observations and dPI:

$$\text{AI}_{cf} = \nu * (\text{PI}_{\text{mod}} - \text{dPI}) \tag{4}$$

$$\rightarrow \mathrm{dAI} = \mathrm{AI_{mod}} * \left(1 - \frac{\mathrm{PI}_{cf}}{\mathrm{PI_{mod}}} \right)$$
$$= \nu * \mathrm{dPI} \tag{5}$$

so that historical dPI is the driver of modern attributable AI changes. We evaluate equations (4) and (5) for each storm over 2019–2023. In cases where storm ν_{mod} values exceed 1.0 but are not superintense (e.g. Persing and Montgomery 2003, Rousseau-Rizzi and Emanuel 2019, approximated as less than $\nu \sim 1.2$), we fix $\nu = 1$ when solving to ensure we do not overestimate the anticipated response. Note that in equation (5) a storm's ν bounds how local attributable intensity changes might respond to local PI changes. This relationship implies that larger absolute dAI values are expected for storms with higher observed AIs (see Sobel *et al* 2016), a key property consistent with empirical evidence that major hurricanes are strengthening in response to climate change faster than weaker storms (Elsner *et al* 2008, Holland and Bruyère 2014, Kossin *et al* 2020). While storm-to-storm variations in dPI clearly affect the final attributability, we find that across our counterfactuals the lower bound on dAI increases with $\mathrm{AI_{mod}}$, as expected (supporting figure S6).
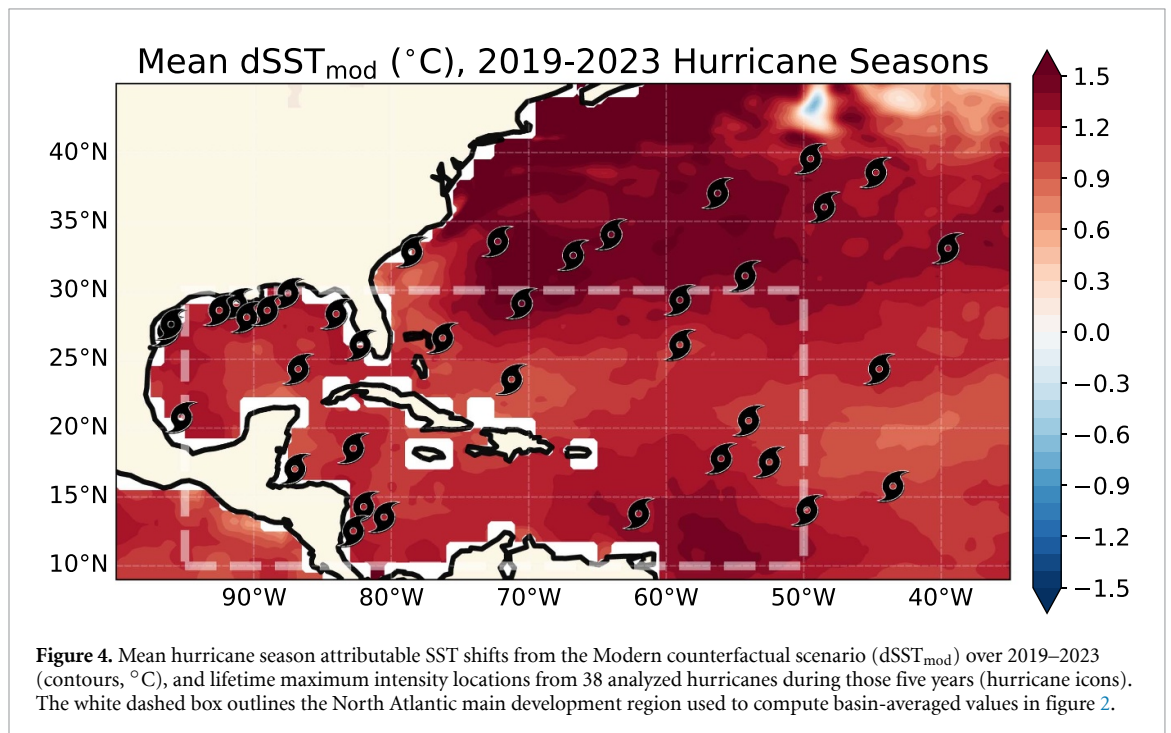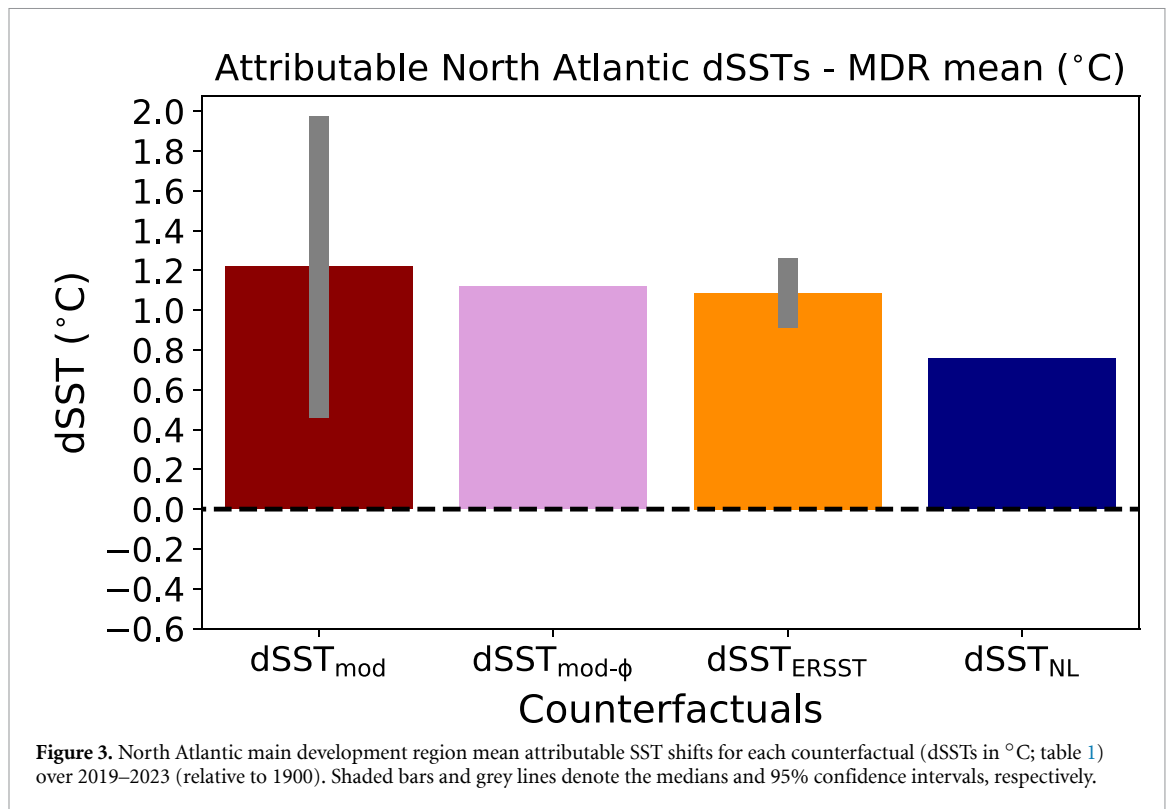
3. Results

3.1. Climate change influences on Atlantic SSTs

Our study considers four counterfactual scenarios: Modern, Zonal-mean Modern, ERSST, and Nonlocally-damped Modern (section 2.2). Each corresponds with a different assumption of how climate change influences hurricane intensity through attributable SST changes.
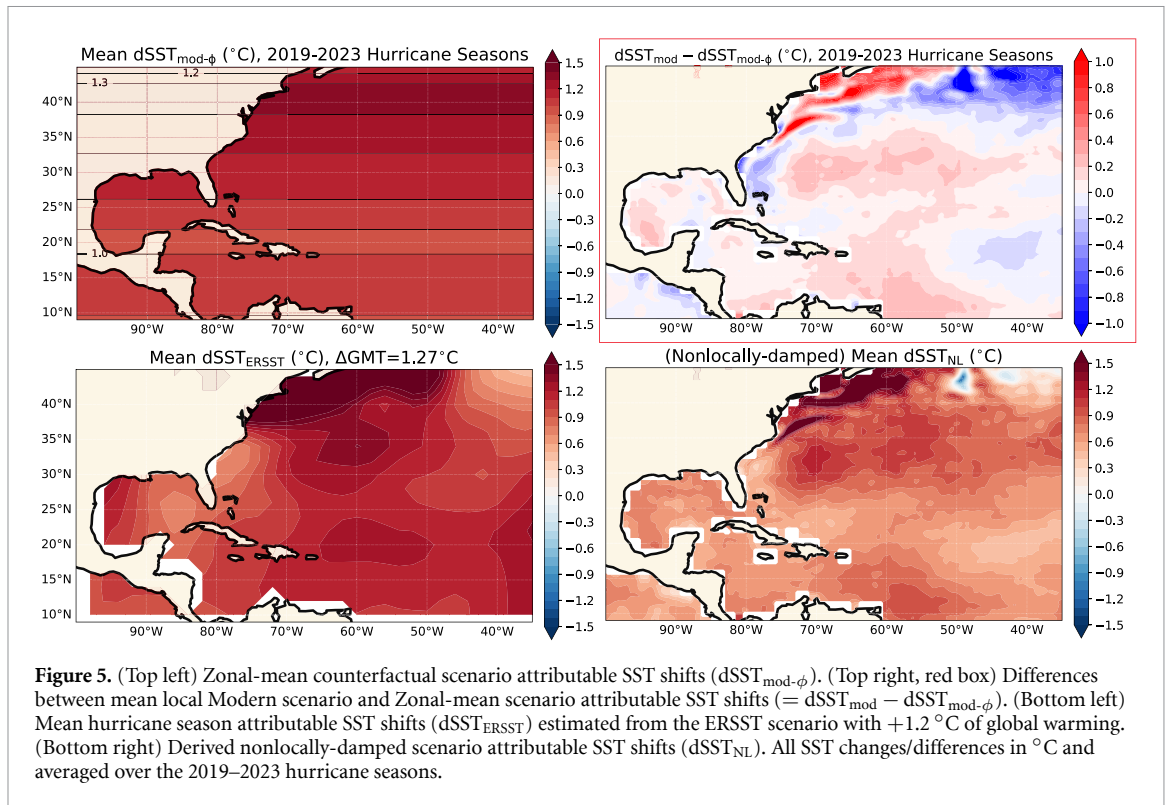
Mean SSTs and mean dSSTs computed over a Gulf/Caribbean-focused main development region definition (figure 3) illustrate each scenario's bulk changes and uncertainties (10–30° N, 95–50° W; white box in figure 4, following Gilford *et al* 2017, other basin definitions have qualitatively similar results). All SSTs have a clear upward trend over the main development region, congruent with the attributable GMT increase since 1900 (figure 2). Trends in OISST and ERSST are strongly related since 1982, but the OISST slope is steeper. The OISST trend acceleration around ~1980 is likely related, in part, to a rebound from reduced anthropogenic aerosol emissions (and accompanying Saharan dust feedbacks) since the 1970s (Rousseau-Rizzi and Emanuel 2021, discussed below).

Mean $\mathrm{dSST_{mod}}$ shifts are $+1.2\,°\mathrm{C}$ across the main development region (figure 3), while $\mathrm{dSST_{ERSST}}$ and $\mathrm{dSST_{zm}}$ are about $0.1\,°\mathrm{C}$ less attributably warm and $\mathrm{dSST_{NL}}$ is about $0.45\,°\mathrm{C}$ less attributably warm. The 95% confidence interval of $\mathrm{dSST_{mod}}$ across the North Atlantic is a considerable fraction of the signal, but still indicates Modern scenario attributable shifts are significantly positive, spanning between $+0.5\,°\mathrm{C}$ and $+2.0\,°\mathrm{C}$ (see confidence intervals in supporting figure S4). The 95% confidence interval of $\mathrm{dSST_{ERSST}}$ is $1.1\,°\mathrm{C}$ narrower than that of $\mathrm{dSST_{mod}}$. This is likely because the number degrees of freedom in the ERSST regression with GMT (i.e. the number of years since 1900) are much higher than in the regression with OISST, and there is no model-based method contribution (along with its uncertainties) used in constructing the ERSST scenario. The overlap between all of the counterfactual scenario averages and their uncertainties imply it is difficult to conclude with confidence which counterfactual North Atlantic SSTs might have followed historically, and which might be most relevant for observed hurricane intensities. Each are plausible depending on the physical and attribution assumptions made. If we overlay the uncertainty bars of the $\mathrm{dSST_{mod}}$ main development region mean on that of $\mathrm{dSST_{NL}}$ (our most conservative considered scenario), we find that the 95% confidence interval does not cross $0\,°\mathrm{C}$ (not shown). This indicates that the attributable SST changes effective for influencing PI (and hence AI) are, on average, significantly $>0\,°\mathrm{C}$ across the full range of counterfactual scenarios considered herein.

Figure 4 shows the average $\mathrm{dSST_{mod}}$ across the North Atlantic over the last 5 hurricane seasons (June–November 2019–2023); this structure is relatively consistent across the six months of hurricane season (supporting figure S3). The Modern counterfactual scenario shows pervasive SST warming across the North Atlantic basin, but there are subtle variations that could matter when encountered by an individual storm during its lifetime; our framework's along-track approach (section 2.3) accounts for this spatial variability. The $\mathrm{dSST_{mod}}$ maxima along $\sim 32°$ N is qualitatively consistent with tropical expansion and poleward increases in PI/observed intensities in response to climate change (e.g. Kossin *et al* 2014, Collins *et al* 2019, Lin *et al* 2023). $\mathrm{dSST_{mod}}$ is commonly $>+1\,°\mathrm{C}$ along the U.S. Gulf coast, where these values are collocated with the LMIs of many landfalling hurricanes over 2019–2023 (though there are seasonal variations in both attributable SSTs and when each storm occurred, supporting figure S3). $\mathrm{dSST_{mod}}$ is also relatively higher in the tropical east Atlantic. Lower $\mathrm{dSST_{mod}}$ ($<+1\,°\mathrm{C}$) values are located in the central North Atlantic, stretching north from Cabo Verde and westward across to the Caribbean, up the southeast Atlantic U.S. coast, and down to the Yucatan. Conspicuously, fewer hurricanes over the last few years appear to have LMIs in these regions of relatively less attributable warming (figure 4).

Figure 3. North Atlantic main development region mean attributable SST shifts for each counterfactual (dSSTs in °C; table 1) over 2019–2023 (relative to 1900). Shaded bars and grey lines denote the medians and 95% confidence intervals, respectively.

Figure 4. Mean hurricane season attributable SST shifts from the Modern counterfactual scenario (dSST$_{mod}$) over 2019–2023 (contours, °C), and lifetime maximum intensity locations from 38 analyzed hurricanes during those five years (hurricane icons). The white dashed box outlines the North Atlantic main development region used to compute basin-averaged values in figure 2.

The hurricane-season-mean spatial structure of the Zonal Mean, ERSST, and Nonlocally-damped scenario dSSTs are plotted for comparison in figure 5. Zonal-mean attributable SSTs (dSST$_{zm}$, top left panel) are narrowly constrained across latitudes: shifts range between $+0.9\,°C$ and $+1.4\,°C$. The resulting spatial structure of the residual between the Modern and Zonal-mean scenarios largely mirrors dSST$_{mod}$ (top right panel; cf figure 4). Coarse attributable SSTs from ERSST (dSST$_{ERSST}$, bottom left panel) are cooler than the Modern scenario in tropical east Atlantic and along the Florida Gulf coast, while they are warmer in the central North Atlantic. dSST$_{ERSST}$ values are also qualitatively consistent with dSST$_{mod}$ values, showing an expansion of the tropics above 30°, relatively low attributable warming in the Caribbean and along the Atlantic southeast coast, and relatively high attributable warming along the western Gulf coast. While shifts
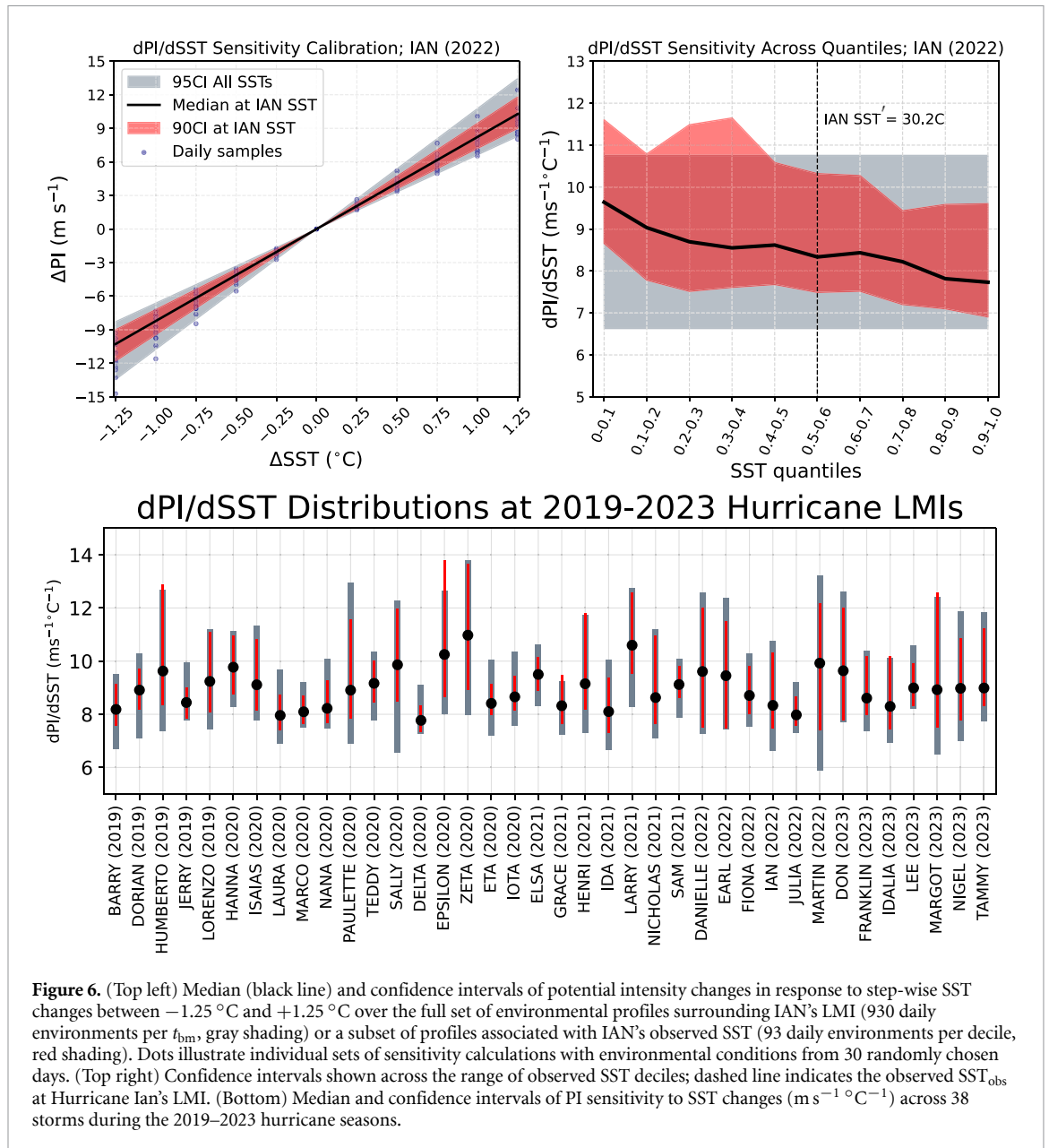
Figure 5. (Top left) Zonal-mean counterfactual scenario attributable SST shifts ($dSST_{mod-\phi}$). (Top right, red box) Differences between mean local Modern scenario and Zonal-mean scenario attributable SST shifts ($= dSST_{mod} - dSST_{mod-\phi}$). (Bottom left) Mean hurricane season attributable SST shifts ($dSST_{ERSST}$) estimated from the ERSST scenario with $+1.2\,°C$ of global warming. (Bottom right) Derived nonlocally-damped scenario attributable SST shifts ($dSST_{NL}$). All SST changes/differences in $°C$ and averaged over the 2019–2023 hurricane seasons.

from the Nonlocally-damped scenario share their spatial structure with $dSST_{mod}$, it is less attributably warm (by definition), with some mean shifts across the central North Atlantic and Caribbean only slightly greater than $0\,°C$.

3.2. Climate change influences on potential intensity

PI changes are highly linear with the stepwise SST perturbations: 98% of the days analyzed across the t_{bm} and locations of hurricane lifetime maximum intensities (1982–2023) have linear fits with $R^2 > 0.95$. Likewise, the standard error of the linear fits averaged across all storms and all days is only $0.13\,\text{ms}^{-1}\,°C^{-1}$ ($<2\%$ of the median slope across all storms). We take the median slope across all days as the model's best estimate, and evaluate the uncertainty in slopes, expressed by σ_{lower} and σ_{upper}, as either a) the 95% confidence interval from assuming the full set of slopes calculated from all 930 daily environments in t_{bm} follows a normal distribution (i.e. $\pm1.96\sigma_{t_{bm}}$, shaded with gray throughout), or b) from the range described by the 5th and 95th percentiles of the subset of profiles in t_{bm} that share a decile with the observed SST at the storm's LMI (shaded with red or dSST colors throughout). These errors represent interannual uncertainties in the local relationship between SSTs and PI either accounting for the full range of environmental conditions (a more conservative and general approach, with relatively larger slope ranges), or a subset of those conditions conditional on their SST decile (a less conservative/more specific approach, with a typically smaller range in slopes), respectively.

Figure 6 illustrates PI sensitivity calculations using Hurricane IAN (2022) as an example, with a median of $8.3\,\text{m s}^{-1}\,°C^{-1}$. Fits between SST step changes (ΔSST) and the responses of PI (ΔPI) demonstrate their strong linear relationship across the climatological set of local environmental conditions. The spread in PI sensitivities conditioned on the observed SST decile (red shading) are narrower than the response to the full range of atmospheric profiles (gray shading), a result consistent across deciles (figure 6, top right panel). While sensitivities and errors vary with SST decile—demonstrating some small nonlinearities as a function of SST_{obs}—$\frac{dPI}{dSST}$ values computed at IAN's LMI remain between ~6.5 and $11.5\,\text{m s}^{-1}\,°C^{-1}$ across the range of climatological profiles IAN could have reasonably historically encountered in the season and location it reached its maximum.

Sensitivity calculations across 2019–2023 hurricanes (bottom panel of figure 6) show that median PI sensitivities to SST are frequently between ~8–$11\,\text{m s}^{-1}\,°C^{-1}$. Sensitivities conditioned on the SST_{obs} decile are generally higher in the open Atlantic, while across the Gulf of Mexico and Caribbean PI sensitivities are lower. Sensitivity errors due to variance in atmospheric conditions generally increase with latitude (supporting figure S4). There appears to be discontinuity across the range of full profile sensitivities for storms with LMIs above $30°\,N$, where $\frac{dPI}{dSST}$ is more tightly restricted to between $7\,\text{m s}^{-1}\,°C^{-1}$ and 12 m

Figure 6. (Top left) Median (black line) and confidence intervals of potential intensity changes in response to step-wise SST changes between −1.25 °C and +1.25 °C over the full set of environmental profiles surrounding IAN's LMI (930 daily environments per t_{bm}, gray shading) or a subset of profiles associated with IAN's observed SST (93 daily environments per decile, red shading). Dots illustrate individual sets of sensitivity calculations with environmental conditions from 30 randomly chosen days. (Top right) Confidence intervals shown across the range of observed SST deciles; dashed line indicates the observed SST_{obs} at Hurricane Ian's LMI. (Bottom) Median and confidence intervals of PI sensitivity to SST changes (m s^{-1} °C^{-1}) across 38 storms during the 2019–2023 hurricane seasons.

s^{-1} °C^{-1} (not shown); this discontinuity could mark the influence of the boundary between tropical and extratropical regimes, but it does not significantly influence results. There are no apparent systematic seasonal dependencies among the $\frac{dPI}{dSST}$ values analyzed in this study.

The PI sensitivities we find are broadly consistent with previous studies that have estimated $\frac{dPI}{dSST}$ with idealized models, global climate models, and theory (Vecchi and Soden 2007, Ramsay and Sobel 2011, Rousseau-Rizzi and Emanuel 2021). In this study we have not explicitly disentangled or assumed either a weak-temperature gradient response or radiative convective equilibrium response to changes in local conditions. Instead we compute PI sensitivities directly from the data, and our results show that empirically-derived local sensitivities from observations are closer to the typical weak-temperature gradient response (~8 m s^{-1} °C^{-1}), but can be larger or smaller than this theoretical weak-temperature gradient slope, depending on season and location.

The attributable human-caused SST shifts applied in this study have particular spatial structures that we consider locally (cf figures 4, 5 and supporting figures S2 and S4). While this is justified because local SSTs are the primary controlling factor in observed North Atlantic potential intensity and hurricane activity (e.g. Emanuel *et al* 2013, Murakami *et al* 2018), the degree to which global forcing can influence the long-term evolution of PI through local SST changes is still an open area of investigation. In each case, locally observed T and q profiles will influence the climatological local sensitivity of PI to SST changes in the modern climate (as expressed in the spread of the quantified sensitivity uncertainties, figure 6). Such environmental

Figure 7. Historical and counterfactual scenario (cf table 1) survival functions of AI distributions for 38 storms analyzed over the 2019–2023 hurricane seasons. Red shading denotes the 95% confidence interval of dAI$_{mod}$ across the distribution of storms. Hurricane IAN's AI$_{mod}$ and dAI are shown with a blue dashed line, for reference.
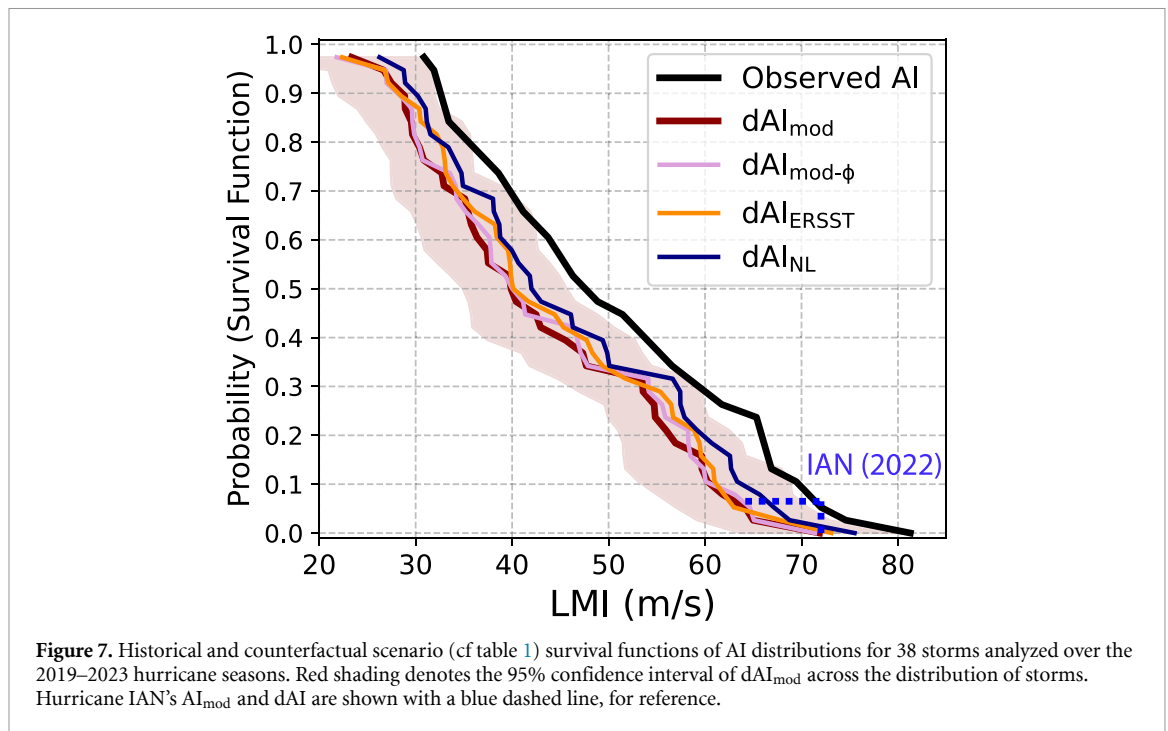
influences are important to consider when computing hurricane intensity responses to SST forcing (Done *et al* 2022). Attributable changes could arise through local forcing (i.e. literally, the warming or moistening of local atmospheric columns due to human-caused climate change), or nonlocally through remote changes in outflow temperatures or a tropics-wide increase in tropospheric saturation moist static energy; each of these could depress PI if they exhibit long-term changes (e.g. Bister and Emanuel 2002, Vecchi and Soden 2007, Rousseau-Rizzi and Emanuel 2021). Our SST-driven approach does not directly account for historical attributable changes in *T* and/or *q* by developing and implementing individual counterfactuals for them. Instead, we address these potentially mitigating influences by (a) using the variability of local environmental profiles to inform sensitivity uncertainties as described here, and by (b) implementing the nonlocally-damped counterfactual, as described above (dSST$_{NL}$, section 2.2). dSST$_{NL}$ indirectly but expressly quantifies how these nonlocal but potentially attributable changes could impact attributable PI through damping from tropics-wide SST warming.

Equation (2) is computed at the time and location of storm's LMI over 2019–2023 (described further below). Combined dPI uncertainties are quantified by resampling from each dSST scenario and $\frac{dPI}{dSST}$ distributions separately (assuming they are normal) with Monte Carlo simulations, recalculating equation (2) with each sample pair, and aggregating. We draw 10 000 sample pairs with replacement and aggregate them to determine the final median and confidence intervals of each counterfactual scenario dPI, for each storm. Because dSST Modern scenario uncertainties are relatively larger than those of PI sensitivities, they tend to dominate the range of Modern dPI responses to historically attributable SST shifts (section 3.3.2).

3.3. Attributable influence on real-world storms

3.3.1. 2019–2023 hurricane seasons

Aggregated survival functions of observed actual intensities and counterfactual AIs (i.e. the probability of an AI being at least a certain value) are shown in figure 7. The Zonal-mean AI$_{cf}$ largely agrees with the Modern AI$_{cf}$, while the ERSST AI$_{cf}$ is slightly faster, and the Nonlocally-damped AI$_{cf}$ is faster still. Each assessed counterfactual intensity, however, falls within the bounds of the Modern AI$_{cf}$ uncertainties (red shading in figure 7). In contrast, our results show a clear emergence of observations from Modern scenario uncertainties across most of the AI distribution, providing statistical evidence that attributably-warmer SSTs intensified many observed hurricanes over 2019–2023.

The full set of Modern scenario dAI and uncertainties are presented in figure 8, alongside the observed AI and Modern AI$_{cf}$ of each storm against Saffir–Simpson categories. For reference we show the mean dAI across all 38 storms (8.3 m s^{-1}) and the mean dAI uncertainty (the storm-by-storm 2σ magnitude; 6.6 m s^{-1}), further demonstrating the robustness of attributability across the set of storms analyzed (and
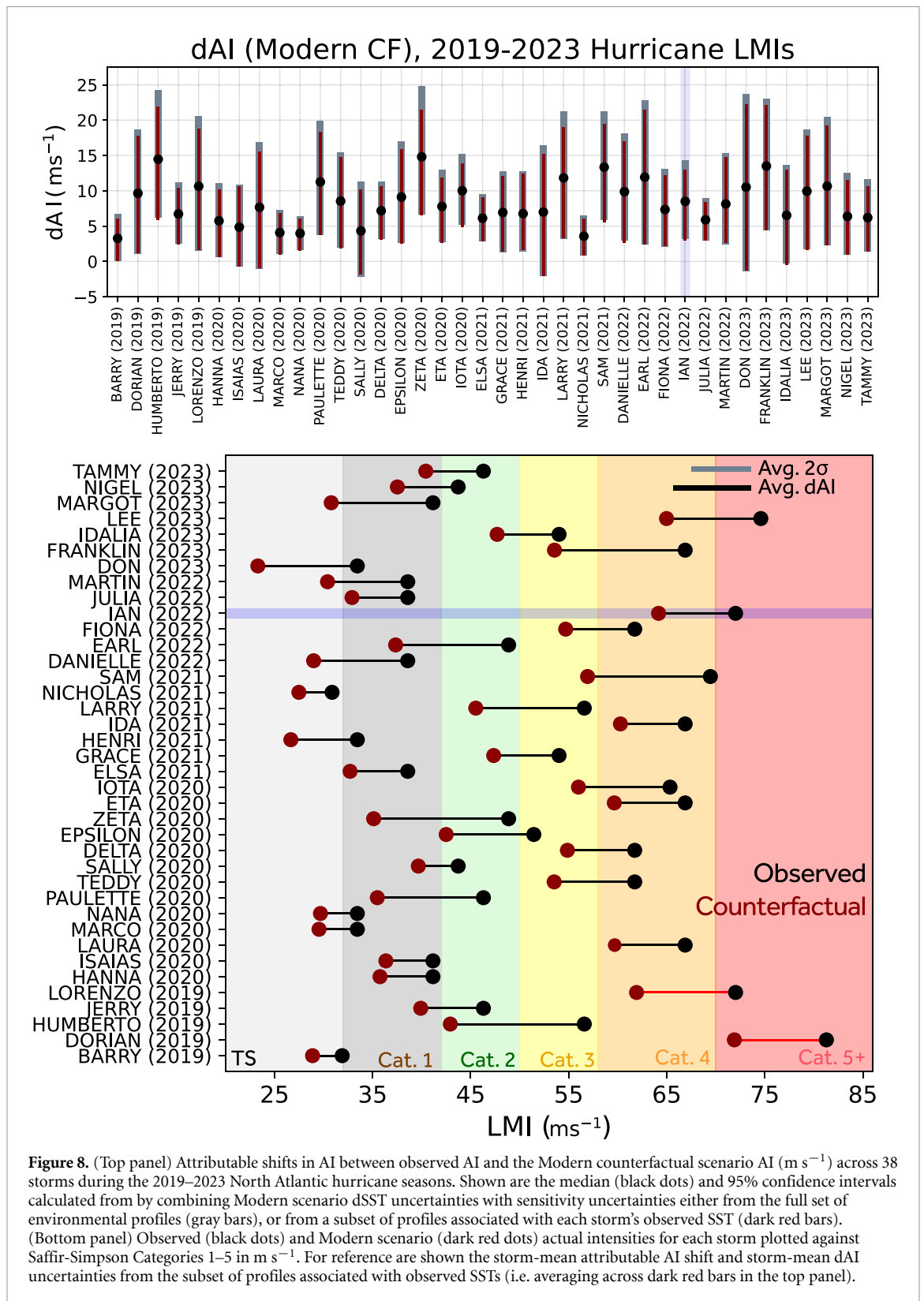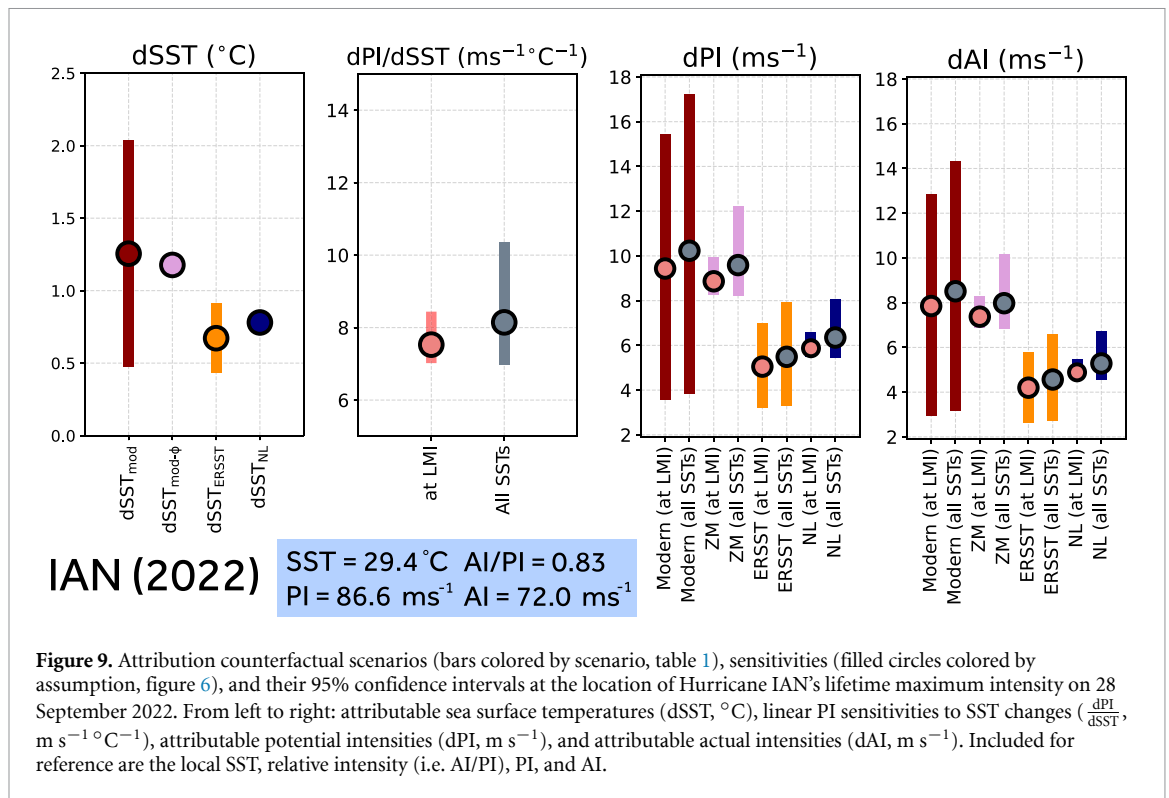
Figure 8. (Top panel) Attributable shifts in AI between observed AI and the Modern counterfactual scenario AI (m s^{-1}) across 38 storms during the 2019–2023 North Atlantic hurricane seasons. Shown are the median (black dots) and 95% confidence intervals calculated from by combining Modern scenario dSST uncertainties with sensitivity uncertainties either from the full set of environmental profiles (gray bars), or from a subset of profiles associated with each storm's observed SST (dark red bars). (Bottom panel) Observed (black dots) and Modern scenario (dark red dots) actual intensities for each storm plotted against Saffir–Simpson Categories 1–5 in m s^{-1}. For reference are shown the storm-mean attributable AI shift and storm-mean dAI uncertainties from the subset of profiles associated with observed SSTs (i.e. averaging across dark red bars in the top panel).

subject our study limitations). Two storms in the dataset exhibited $\nu > 1.0$ (red lines in figure 8, bottom panel); their inclusion does not qualitatively affect our results.

The majority of storms have a Modern scenario median dAI between 6 and 10 m s^{-1}. BARRY (2019) has the lowest median estimate (3.3 m s^{-1}) and ZETA (2020) has the largest median estimate (14.8 m s^{-1}). DON (2023) displays the largest uncertainty, with its 95% confidence interval (across its full set of daily environments) spanning over 25 m s^{-1}. NANA (2020) has the most tightly constrained set of attributable estimates, with a Modern dAI falling between 1.7 and 6.5 m s^{-1}. While the contributions to uncertainty from

Figure 9. Attribution counterfactual scenarios (bars colored by scenario, table 1), sensitivities (filled circles colored by assumption, figure 6), and their 95% confidence intervals at the location of Hurricane IAN's lifetime maximum intensity on 28 September 2022. From left to right: attributable sea surface temperatures (dSST, °C), linear PI sensitivities to SST changes ($\frac{dPI}{dSST}$, m s^{-1} °C^{-1}), attributable potential intensities (dPI, m s^{-1}), and attributable actual intensities (dAI, m s^{-1}). Included for reference are the local SST, relative intensity (i.e. AI/PI), PI, and AI.

attributable SST shifts and PI sensitivities vary from storm to storm, SST-scenario uncertainties principally control the range in dAI estimates; this is evidenced by the minimal differences between results from the full set and SST-decile subset of environmental conditions in final dAI estimates.

Across the 38 storms studied, 30 (79%) have a Modern AI$_{cf}$ that is a category lower than their observed maximum AI. This is partially happenstance, because it depends on how far into a category's definition each storm's original AI is found. However, the average dAI across all storms (8.3 m s^{-1}) is very close to the average width of each bounded category definition (~8.25 m s^{-1} between Categories 1–4), enabling the calculated dAI to frequently move a storm from a higher category in observations to a lower category in the estimated counterfactual scenario.

3.3.2. Hurricane IAN (2022) case study

Figure 9 shows the SST-driven attribution analysis at Hurricane IAN's LMI (28 Sept. 2022, 82.75° W, 26° N). IAN reached its maximum intensity in the band of attributably warmer SSTs along the U.S. Gulf coast (supporting figure 1). Median attributable SST shifts at IAN's LMI range between 0.6 and 1.3 °C, with a high-end Modern scenario estimate breaching >2 °C. IAN's LMI is located near the regional minima of attributable ERSST shifts (figure 5), leading to a lower-bound estimate of ~0.45 °C from the ERSST scenario. The Zonal-mean dSST scenario estimate is consistent with (and less warm than) the Modern scenario, while the Nonlocally-damped scenario is slightly warmer than ERSST's attributable shift.

Paired with these above-storm-average attributable SST shifts at the time and location of IAN's LMI (compared with the full set of 38 storms over 2019–2023, section 3.3.1) is a below-storm-average local PI sensitivity to SSTs (cf figure 6). The Caribbean and Gulf of Mexico consistently have the lowest PI sensitivities to SST changes among those calculated, which constrains IAN's PI sensitivity to between 7–10 m s^{-1} °C^{-1}.

Altogether, despite being the third-most intense storm over the last five years, IAN has a moderate attributable change in intensity due to SST shifts, with a mean dAI between 4 and 8.5 m s^{-1} across the counterfactual scenarios. The total uncertainty in IAN's dAI is dominated by the uncertainties contributed by dSST$_{mod}$, with attributable intensity shifts spanning over 3–14 m s^{-1}. Notably, across the range of scenarios these shifts emerge from the uncertainty (cf figure 7), being significantly greater than 0 m s^{-1}, indicating that historically attributable SSTs robustly increased Hurricane IAN's intensity by *at least* 4% (and possibly up to 21%).

4. Discussion

This work has used an SST-based strategy, primarily considering how local North Atlantic attributable changes in SSTs have influenced actual hurricane intensities through potential intensity theory. But other local and nonlocal factors beyond our scope may also have influenced attributable changes in hurricane intensities since pre-industrial. Changes in atmospheric circulation or hurricane wind shear, for instance, could be correlated with warming and ultimately influence how PI relates to actual intensities, or affect the magnitude of the PI response itself through changes in surface winds (Zhang and Delworth 2009, Emanuel *et al* 2013). Oceanic feedback between hurricane activity and *in-situ* SST cooling could limit the final influences of attributable SST changes (e.g. Lloyd and Vecchi 2011). An historically-attributable poleward migration of storms could also offset intensity increases in the Atlantic (Kossin *et al* 2014, Lin *et al* 2023), but track shifts have not been considered in this work's univariate storyline attribution approach.

A limitation of this study is that it has not comprehensively assessed how nonlocal atmospheric responses to global warming could influence hurricane attribution estimates. The framework relies on local absolute SST changes, rather than North Atlantic SST changes relative to the rest of the tropics, to drive attributable computations. Nonlocal historical changes in the moist static energy content of the tropical troposphere could act to reduce PI's sensitivity to local SST changes, damping the resulting response to local attributable SST changes (Vecchi and Soden 2007, Ramsay and Sobel 2011, Rousseau-Rizzi and Emanuel 2021). The Nonlocally-damped scenario employed in this work makes a simplified adjustment to the modern counterfactual to implicitly account for nonlocal damping through correlation with the tropical atmosphere response, following (Swanson 2008). The median estimate of nonlocally-damped attributable potential intensity changes is 7.2 m s^{-1} (on average) across 2019–2023 storms, ~63% of the median PI response in the Modern scenario (11.5 m s^{-1}). If the local PI response to global warming was perfectly damped in an idealized climate, then PI sensitivity might be expected to follow a radiative convective equilibrium response, ~15%–20% of the transient weak-temperature gradient response (which the empirically-derived sensitivities found herein are more closely aligned with). The mismatch suggests that either the attribution framework is underestimating the magnitude of nonlocal damping from historical tropical-mean changes, or that the real atmosphere is responding different from idealized modeling—transiently adjusting such that nonlocal and local affects are difficult to disentangle with the empirical sensitivity approach—or some degree of both. Future improvements to the attribution framework should consider these possibilities.

Atmospheric aerosols play a subtle role in our methodology and results. Aerosol-driven cooling and a Saharan-dust feedback are known to have affected Atlantic SST variability and trends during the second half of the 20th century (Booth *et al* 2012, Murakami *et al* 2018, Rousseau-Rizzi and Emanuel 2022). An aerosol-driven SST warming trend since ~1980 could mask the attributable magnitude and spatial signal of greenhouse gas warming on Atlantic SSTs. This study addresses the potentially confounding signals of aerosols and global warming in two ways. First, aerosol emissions are implicitly included in the expression of anthropogenic forcing on Atlantic SSTs, i.e. the aerosol signal—and the associated attributable evolution of SSTs over time and space—is *not* explicitly separated from the human emissions considered by the attribution framework (e.g. Murakami *et al* 2020). In this way, local aerosol influences are considered attributable in the same respect that greenhouse gas influences are. Second, an ERSST counterfactual scenario is developed and applied to directly consider SST correlations with global temperature over every year since 1900, wholly encompassing the temperature depression and rebound from mid-century human-made aerosol emissions. Comparison between the Modern and ERSST scenarios reveal the spatial structure of departures between recent and long-term trends, highlighting where aerosol-rebound warming may play an outsized role in present-day attribution assessment. Differences are most apparent in the Gulf of Mexico and southern portion of the eastern tropical Atlantic. Future work could explicitly separate and further investigate these influences.

5. Conclusions

This study has proposed and applied a novel framework to rapidly assess attributable changes in North Atlantic hurricane intensities due to attributable SST changes since the pre-industrial period. Counterfactual scenarios of local attributable SSTs developed from recently published multi-method attribution analyses (Giguere *et al* 2024) are combined with empirical estimates of potential intensity sensitivity to SST, in order to estimate attributable PI changes due to various representations of attributable SST warming. The robust statistical relationship between actual and potential intensities (e.g. Emanuel 2000, Gilford *et al* 2019) is leveraged to calculate the SST-driven attributability of hurricane intensities (see Sobel *et al* 2016, Sparks and Toumi 2024). The behavior and results from this rapid attribution framework are illustrated with observed storms from five recent hurricane seasons, 2019–2023. The resulting attributable intensity changes at the

location and times of storm lifetime maximums indicate that there are robust and detectable SST-warming influences on recent observed North Atlantic hurricane intensities—a trend expected to continue in the hurricane seasons to come.

Analyses of 38 hurricanes over the 2019–2023 hurricane seasons show that modern storms are ~8.3 m s^{-1} (about a category) more intense, on average, than they would have been in a world without human-driven North Atlantic SST warming. While the mean attributable SST influence varies from storm to storm based on their location and season, uncertainty analysis show hurricane intensities are robustly increasing: 32 of the 38 storms studied (84%) have SST-driven attributable intensity changes significantly >0 m s^{-1}. Nine of the storms studied have 95% confidence interval upper bounds on attributable intensity changes that exceed $+20$ m s^{-1}; in these 'highest-case' scenarios, climate change could have increased these storm's intensities by at least two categories, compared to what they would have been in a cooler counterfactual world.

The attributable shifts and uncertainties for any given storm's intensity depends on the PI sensitivities and historically-observed or modeled SST changes at the location and time where the storm reached it maximum. Nevertheless, SST-driven attributable increases in recent hurricane intensities are *generally* highest for the most intense storms. Taken together with increasing SST attributability (as GMT continues to rise), this study's results are consistent with recent historical analyses finding that major hurricanes are becoming more common (Kossin *et al* 2020). Several recent storms had large median attributable increases of ~14–15 m s^{-1}, including hurricanes HUMBERTO (2019), ZETA (2020), and FRANKLIN (2023).

The storyline attribution approach used here permits a close examination of how different expressions of SST distribution shifts could distinctly influence individual hurricane intensities. Four counterfactual scenarios were considered, together designed to investigate the range of possibilities for how North Atlantic hurricane intensities might respond to SST warming caused by global climate change. The baseline Modern counterfactual scenario is based on the published findings of Giguere *et al* (2024), using linear empirical estimates from OISST (1982–2021) combined with climate model outputs to estimate the spatially-resolved mean SST shifts and uncertainties since 1900. Results from the Modern scenario have the largest attributable changes, but also have large uncertainties. The Zonal-mean counterfactual scenario takes the global zonal-mean of attributable SSTs from the Modern counterfactual, an approach more consistent with global climate forcing; its results are often difficult to distinguish from the Modern scenario, but it generally has slightly cooler attributable SST shifts (especially in the Caribbean). The ERSST scenario uses linear empirical estimates from a long-term SST dataset (1900–2021); results are coarser and weaker than the Modern baseline, but tend to have smaller uncertainties because of the longer period over which the underlying regression between SST and GMT is performed. Finally, the Nonlocally-damped scenario is based on the Modern scenario, but reduces its magnitude as a first order estimate accounting for nonlocal damping processes, following Swanson (2008). Nonlocally-damped attributable SST shifts are ~0.45° cooler than the Modern scenario, leading to attributable intensity shifts that are ~35% weaker (on average).

The SST-driven tropical cyclone intensity attribution framework introduced here provides a roadmap for producing rapid, quantified, and robust attribution estimates of hurricane intensities to support timely climate communications. To expand communications globally and permit more broadly applicable analyses, future studies are planned to apply this framework to other ocean basins. Subdividing and comparing attribution estimates between landfalling and open ocean storms could inform the extent to which increasingly intense hurricanes could affect populated coastlines and communities (Levin and Murakami 2019, Vecchi *et al* 2021). Quantifying and communicating the extent to which tropical cyclone intensities are attributable will ultimately enable stakeholders and the general public to more readily connect the dots between human-caused climate change and intense storms when they arise (Osaka and Bellamy 2020, McClure *et al* 2022, Thomas-Walters *et al* 2024).

Data availability statement

Regridding was performed with the `xesmf` package (Zhuang *et al* 2023). Analysis notebooks and output data will be available on Zenodo at https://doi.org/10.5281/zenodo.12706456 upon publication.

Data and code supporting the findings of this study are openly available at: https://doi.org/10.5281/zenodo.12706456.

Acknowledgments

ORCID iDs

Daniel M Gilford ● https://orcid.org/0000-0003-2422-0887
Joseph Giguere ● https://orcid.org/0009-0008-8734-4880
Andrew J Pershing ● https://orcid.org/0000-0003-4432-0850

References

Arnold M V, Dewhurst D R, Alshaabi T, Minot J R, Adams J L, Danforth C M and Dodds P S 2021 Hurricanes and hashtags: characterizing online collective attention for natural disasters *PLoS One* **16** e0251762

Birkland T A 1998 Focusing events, mobilization and agenda setting *J. Public Policy* **18** 53–74

Bister M and Emanuel K A 1998 Dissipative heating and hurricane intensity *Meteorol. Atmos. Phys.* **65** 233–40

Bister M and Emanuel K A 2002 Low frequency variability of tropical cyclone potential intensity 1. Interannual to interdecadal variability *J. Geophys. Res. Atmos.* **107** ACL 26-1-ACL 26-15

Booth B B B, Dunstone N J, Halloran P R, Andrews T and Bellouin N 2012 Aerosols implicated as a prime driver of twentieth-century North Atlantic climate variability *Nature* **484** 228–32

Boudet H, Giordono L, Zanocco C, Satein H and Whitley H 2020 Event attribution and partisanship shape local discussion of climate change after extreme weather *Nat. Clim. Change* **10** 69–76

Carver R W and Merose A 2023 4A.1—ARCO-ERA5: an analysis-ready cloud-optimized reanalysis dataset *22nd Conf. on AI for Env. Science (Denver, CO)* (American Meteorological Society)

Cody E M, Stephens J C, Bagrow J P, Dodds P S and Danforth C M 2017 Transitions in climate and energy discourse between Hurricanes Katrina and Sandy *J. Environ. Stud. Sci.* **7** 87–101

Collins M *et al* 2019 Extremes, abrupt changes and managing risk *IPCC Special Report on the Ocean and Cryosphere in a Changing Climate* ed H O Pörtner *et al* (Cambridge University Press) pp 589–655

Done J M, Lackmann G M and Prein A F 2022 The response of tropical cyclone intensity to changes in environmental temperature *Weather Clim. Dyn.* **3** 693–711

Elsner J B, Kossin J P and Jagger T H 2008 The increasing intensity of the strongest tropical cyclones *Nature* **455** 92–95

Emanuel K A 1986 An air-sea interaction theory for tropical cyclones. Part I: steady-state maintenance *J. Atmos. Sci.* **43** 585–605

Emanuel K A 1987 The dependence of hurricane intensity on climate *Nature* **326** 483–5

Emanuel K A 2005 Increasing destructiveness of tropical cyclones over the past 30 years *Nature* **436** 686–8

Emanuel K 2000 A statistical analysis of tropical cyclone intensity *Mon. Weather Rev.* **128** 1139–52

Emanuel K 2011 Global warming effects on U.S. hurricane damage *Weather Clim. Soc.* **3** 261–8

Emanuel K, Solomon S, Folini D, Davis S and Cagnazzo C 2013 Influence of tropical tropopause layer cooling on Atlantic hurricane activity *J. Clim.* **26** 2288–301

Ettinger J, Walton P, Painter J, Osaka S and Otto F E L 2021 "What's up with the weather?" Public engagement with extreme event attribution in the United Kingdom *Weather Clim. Soc.* **13** 341–52

Evan A T, Vimont D J, Heidinger A K, Kossin J P and Bennartz R 2009 The role of aerosols in the evolution of tropical North Atlantic Ocean temperature anomalies *Science* **324** 778–81

Eyring V, Bony S, Meehl G A, Senior C A, Stevens B, Stouffer R J and Taylor K E 2016 Overview of the coupled model intercomparison project phase 6 (CMIP6) experimental design and organization *Geosci. Model Dev.* **9** 1937–58

Eyring V *et al* 2021 Human influence on the climate system *Climate Change 2021: The Physical Science Basis. Contribution of Working Group I to the Sixth Assessment Report of the Intergovernmental Panel on Climate Change* ed T Halenka, J A Marengo Orsini and D Mitchell (Cambridge University Press)

Giguere J, Gilford D M and Pershing A 2024 Attributing daily ocean temperatures to anthropogenic climate change *Environ. Res. Clim.* **3** 035003

Gilford D M 2021 pyPI (v1.3): Tropical Cyclone Potential Intensity Calculations in Python *Geosci. Model Dev.* **14** 2351–69

Gilford D M, Pershing A, Strauss B H, Haustein K and Otto F E L 2022 A multi-method framework for global real-time climate attribution *Adv. Stat. Clim. Meteorol. Oceanogr.* **8** 135–54

Gilford D M, Solomon S and Emanuel K A 2017 On the seasonal cycles of tropical cyclone potential intensity *J. Clim.* **30** 6085–96

Gilford D M, Solomon S and Emanuel K A 2019 Seasonal cycles of along-track tropical cyclone maximum intensity *Mon. Weather Rev.* **147** 2417–32

Gilford D 2020 dgilford/pyPI: pyPI v1.3 (initial package release) *Zenodo* https://doi.org/10.5281/zenodo.3985975

Holland G and Bruyère C L 2014 Recent intense hurricane response to global climate change *Clim. Dyn.* **42** 617–27

Huang B, Banzon V F, Freeman E, Lawrimore J, Liu W, Peterson T C, Smith T M, Thorne P W, Woodruff S D and Zhang H-M 2015 Extended reconstructed sea surface temperature version 4 (ERSST.v4). Part I: upgrades and intercomparisons *J. Clim.* **28** 911–30

Huang B, Thorne P W, Banzon V F, Boyer T, Chepurin G, Lawrimore J H, Menne M J, Smith T M, Vose R S and Zhang H M 2017 NOAA extended reconstructed sea surface temperature (ERSST), version 5 (NOAA National Centers for Environmental Information) (https://doi.org/10.7289/V5T72FNM) (Accessed 25 September 2023)

Knapp K R, Diamond H J, Kossin J P, Kruk M C and Schreck C J 2018 International best track archive for climate stewardship (IBTrACS) project, version 4 [North Atlantic data: IBTrACS.na.v04r00.nc] (NOAA National Centers for Environmental Information) (Accessed 8 February 2024)

Knapp K R, Kruk M C, Levinson D H, Diamond H J and Neumann C J 2010 The international best track archive for climate stewardship (IBTrACS) *Bull. Am. Meteorol. Soc.* **91** 363–76

Knutson T *et al* 2019 Tropical cyclones and climate change assessment *Bull. Am. Meteorol. Soc.* **100** 1987–2007

Kossin J P, Emanuel K A and Vecchi G A 2014 The poleward migration of the location of tropical cyclone maximum intensity *Nature* **509** 349–52

Kossin J P, Knapp K R, Olander T L and Velden C S 2020 Global increase in major tropical cyclone exceedance probability over the past 40 years *Proc. Natl Acad. Sci.* **117** 11975–80

Lackmann G M 2015 Hurricane Sandy before 1900 and after 2100 *Bull. Am. Meteorol. Soc.* **96** 547–60

Lange S 2019 Trend-preserving bias adjustment and statistical downscaling with ISIMIP3BASD (v1.0) *Geosci. Model Dev.* **12** 3055–70

Levin E L and Murakami H 2019 Impact of anthropogenic climate change on United States major hurricane landfall frequency *J. Mar. Sci. Eng.* **7** 135

Lin I-I, Camargo S J, Lien C-C, Shi C-A and Kossin J P 2023 Poleward migration as global warming's possible self-regulator to restrain future western North Pacific Tropical Cyclone's intensification *npj Clim. Atmos. Sci.* **6** 34

Lloyd E A and Oreskes N 2018 Climate change attribution: when is it appropriate to accept new methods? *Earth's Future* **6** 311–25

Lloyd I D and Vecchi G A 2011 Observational evidence for oceanic controls on hurricane intensity *J. Clim.* **24** 1138–53

Masson-Delmotte V *et al* 2021 *Climate Change 2021: The Physical Science Basis. Contribution of Working Group I to the Sixth Assessment Report of the Intergovernmental Panel on Climate Change* (Cambridge University Press)

McClure J, Noy I, Kashima Y and Milfont T L 2022 Attributions for extreme weather events: science and the people *Clim. Change* **174** 22

Murakami H *et al* 2020 Detected climatic change in global distribution of tropical cyclones *Proc. Natl Acad. Sci.* **117** 10706–14

Murakami H, Levin E, Delworth T L, Gudgel R and Hsu P-C 2018 Dominant effect of relative tropical Atlantic warming on major hurricane occurrence *Science* **362** 794–9

National Academies of Sciences 2016 *Attribution of Extreme Weather Events in the Context of Climate Change* (The National Academies Press)

Nordhaus W D 2010 The economics of hurricanes and implications of global warming *Clim. Change Econ.* **1** 1–20

Ogunbode C A, Demski C, Capstick S B and Sposato R G 2019 Attribution matters: revisiting the link between extreme weather experience and climate change mitigation responses *Glob. Environ. Change* **54** 31–39

Osaka S and Bellamy R 2020 Natural variability or climate change? Stakeholder and citizen perceptions of extreme event attribution *Glob. Environ. Change* **62** 102070

Patricola C M and Wehner M F 2018 Anthropogenic influences on major tropical cyclone events *Nature* **563** 339–46

Persing J and Montgomery M T 2003 Hurricane superintensity *J. Atmos. Sci.* **60** 2349–71

Pfleiderer P, Nath S and Schleussner C-F 2022 Extreme Atlantic hurricane seasons made twice as likely by ocean warming *Weather Clim. Dyn.* **3** 471–82

Philip S *et al* 2020 A protocol for probabilistic extreme event attribution analyses *Adv. Stat. Climatol. Meteorol. Oceanogr.* **6** 177–203

Ramsay H A and Sobel A H 2011 Effects of relative and absolute sea surface temperature on tropical cyclone potential intensity using a single-column model *J. Clim.* **24** 183–93

Reed K A and Wehner M F 2023 Real-time attribution of the influence of climate change on extreme weather events: a storyline case study of Hurricane Ian rainfall *Environ. Res. Clim.* **2** 043001

Reed K A, Wehner M F, Stansfield A M and Zarzycki C M 2021 Anthropogenic influence on Hurricane Dorian's extreme rainfall *Bull. Am. Meteorol. Soc.* **102** S9–S16

Reynolds R W, Rayner N A, Smith T M, Stokes D C and Wang W 2002 An improved *in situ* and satellite SST analysis for climate *J. Clim.* **15** 1609–25

Rousseau-Rizzi R and Emanuel K 2019 An evaluation of hurricane superintensity in axisymmetric numerical models *J. Atmos. Sci.* **76** 1697–708

Rousseau-Rizzi R and Emanuel K 2021 A weak temperature gradient framework to quantify the causes of potential intensity variability in the tropics *J. Clim.* **34** 8669–82

Rousseau-Rizzi R and Emanuel K 2022 Natural and anthropogenic contributions to the hurricane drought of the 1970s–1980s *Nat. Commun.* **13** 1–10

Schiermeier Q 2008 Hurricanes are getting fiercer *Nature* (https://doi.org/10.1038/news.2008.1079)

Schmidt S, Kemfert C and Höppe P 2009 Tropical cyclone losses in the USA and the impact of climate change—a trend analysis based on data from a new approach to adjusting storm losses *Environ. Impact Assess. Rev.* **29** 359–69

Seneviratne S *et al* 2021 Weather and climate extreme events in a changing climate *Climate Change 2021: The Physical Science Basis. Contribution of Working Group I to the Sixth Assessment Report of the Intergovernmental Panel on Climate Change* ed V Masson-Delmotte *et al* (Cambridge University Press) pp 1513–766

Shen W, Tuleya R E and Ginis I 2000 A sensitivity study of the thermodynamic environment on GFDL model hurricane intensity: implications for global warming *J. Clim.* **13** 109–21

Shepherd T G 2016 A common framework for approaches to extreme event attribution *Curr. Clim. Change Rep.* **2** 28–38

Shepherd T G *et al* 2018 Storylines: an alternative approach to representing uncertainty in physical aspects of climate change *Clim. Change* **151** 555–71

Silver A and Jackson S 2023 Public attention during Hurricanes Florence and Michael *Weather Clim. Soc.* **15** 425–35

Sobel A H, Camargo S J, Hall T M, Lee C-Y, Tippett M K and Wing A A 2016 Human influence on tropical cyclone intensity *Science* **353** 242–6

Sparks N and Toumi R 2024 IRIS : the Imperial College storm model *Sci. Data* **11** 8–10

Strauss B H, Orton P M, Bittermann K, Buchanan M K, Gilford D M, Kopp R E, Kulp S, Massey C, de Moel H and Vinogradov S 2021 Economic damages from Hurricane Sandy attributable to sea level rise caused by anthropogenic climate change *Nat. Commun.* **12** 1–9

Swain D L, Singh D, Touma D and Diffenbaugh N S 2020 Attributing extreme events to climate change: a new frontier in a warming world *One Earth* **2** 522–7

Swanson K L 2008 Nonlocality of Atlantic tropical cyclone intensities *Geochem. Geophys. Geosyst.* **9** Q04V01

Thomas-Walters L, Goldberg M H, Lee S, Lyde A, Rosenthal S A and Leiserowitz A 2024 Communicating the links between climate change and heat waves with the climate shift index *Weather Clim. Soc.* **16** 511–20

Trenary L, DelSole T, Camargo S J and Tippett M K 2019 Are midtwentieth century forced changes in North Atlantic hurricane potential intensity detectable? *Geophys. Res. Lett.* **46** 3378–86

Trenberth K E, Cheng L, Jacobs P, Zhang Y and Fasullo J 2018 Hurricane Harvey links to ocean heat content and climate change adaptation *Earth's Future* **6** 730–44

van Oldenborgh G J *et al* 2021 Pathways and pitfalls in extreme event attribution *Clim. Change* **166** 13

Van Oldenborgh G J, Van Der Wiel K, Sebastian A, Singh R, Arrighi J, Otto F, Haustein K, Li S, Vecchi G and Cullen H 2017 Attribution of extreme rainfall from Hurricane Harvey, August 2017 *Environ. Res. Lett.* **12** 124009

Vecchi G A, Landsea C, Zhang W, Villarini G and Knutson T 2021 Changes in Atlantic major hurricane frequency since the late-19th century *Nat. Commun.* **12** 1–9

Vecchi G A and Soden B J 2007 Effect of remote sea surface temperature change on tropical cyclone potential intensity *Nature* **450** 1066–70

Vecchi G A, Swanson K L and Soden B J 2008 Climate change: whither hurricane activity? *Science* **322** 687–9

Wang S-Y S, Zhao L, Yoon J-H, Klotzbach P and Gillies R R 2018 Quantitative attribution of climate effects on Hurricane Harvey's extreme rainfall in Texas *Environ. Res. Lett.* **13** 054014

Wehner M F and Kossin J P 2024 The growing inadequacy of an open-ended Saffir-Simpson hurricane wind scale in a warming world *Proc. Natl Acad. Sci. USA* **121** 1–7

Wehner M F and Reed K A 2022 Operational extreme weather event attribution can quantify climate change loss and damages *PLOS Clim.* **1** 1–4

Wehner M F, Zarzycki C and Patricola C 2019 Estimating the human influence on tropical cyclone intensity as the climate changes *Hurricane Risk* ed J M Collins and K Walsh (Springer) pp 235–60

Wing A A, Emanuel K and Solomon S 2015 On the factors affecting trends and variability in tropical cyclone potential intensity *Geophys. Res. Lett.* **42** 8669–77

Wong-Parodi G and Garfin D R 2022 Hurricane adaptation behaviors in Texas and Florida: exploring the roles of negative personal experience and subjective attribution to climate change *Environ. Res. Lett.* **17** 034033

Zanocco C, Mote P, Flora J and Boudet H 2024 Comparing public and scientific extreme event attribution to climate change *Clim. Change* **177** 76

Zeng Z, Wang Y and Wu C-C 2007 Environmental dynamical control of tropical cyclone intensity—an observational study *Mon. Weather Rev.* **135** 38–59

Zhang R and Delworth T L 2009 A new method for attributing climate variations over the Atlantic Hurricane Basin's main development region *Geophys. Res. Lett.* **36** 1–5

Zhuang J *et al* 2023 pangeo-data/xesmf: v0.7.1 *Zenodo* https://doi.org/10.5281/zenodo.7800141